Anisotropic Strain Enhanced Hydrogen Solubility in bcc Metals: The Independence on the Sign of Strain

Hong-Bo Zhou, Shuo Jin, Ying Zhang, Guang-Hong Lu, and Feng Liu

Phys. Rev. Lett. **109**, 135502 — Published 27 September 2012

DOI: 10.1103/PhysRevLett.109.135502

Anisotropic Strain Enhanced Hydrogen Solubility in bcc Metals: The Independence on the Sign of Strain

Hong-Bo Zhou, Shuo Jin, Ying Zhang, and Guang-Hong Lu*

Department of Physics, Beihang University, Beijing 100191, China

Feng Liu

Department of Materials Science and Engineering, University of Utah, Salt Lake City, Utah 84112, USA

When an impurity is doped in a solid, it inevitably induces a local stress, tending to expand or contract the lattice. Consequently, strain can be applied to change the solubility of impurity in a solid. Generally the solubility responds to strain "monotonically", increasing (decreasing) with the tensile (compressive) strain if the impurity induces a compressive stress or vice versa. Using first-principles calculations, however, we discovered that the H solubility can be enhanced by anisotropic strain in some bcc metals, almost independent of the sign of strain. This anomalous behavior is found to be caused by a continuous change of H location induced by anisotropic strain. Our finding suggests a cascading effect of H bubble formation in bcc metals: the H solution leads to H bubble formation that induces anisotropic strain that in turn enhances H solubility to further facilitate bubble growth.

PACS number(s): 62.20.-x, 81.05.Bx, 61.72.S-

The solubility of impurity in solids is of not only scientific interest but also technological importance [1]. Strain engineering has been recognized to provide an effective way to enhance the solubility of impurity in solids, such as doping of impurity in semiconductors. In general, the impurity formation energy is a linear monotonic function of strain following elasticity theory, no matter a hydrostatic or biaxial strain [2, 3]. Thus, one can expect when a "large" impurity induces a compressive lattice stress, tending to expand the lattice, its solubility can only be enhanced by applying a tensile strain but decreased by a compressive strain; and the reverse is true for a "small" impurity. In this Letter, we report the discovery of an exceptional case that the H solubility in some bcc metals is found to be enhanced by applying both a tensile and compressive anisotropic strain, independent of the sign of strain. This surprising counter-intuitive behavior is shown to be caused by an unusual strain induced continuous change of H minimum-energy location from one interstitial site to another.

Hydrogen is the most common impurity in metals. Understanding the H solubility in metals has broad and significant technological implications. Hydrogen retention assists vacancy formation in many metals that degrades their structural properties, a phenomenon known as H embrittlement [4-6]. Metal hydrides have been intensively studied for H storage [7, 8]. In a fusion reactor, metals are used as the plasma facing material (PFM) that is exposed to extremely high fluxes of H isotope (deuterium–tritium) ions [9]. The accumulation of H in metals leads to formation of voids, bubbles, and blisters [10]. In this regard, our finding suggests a cascading

effect of H bubble formation in bcc metals, which has significant implications in using bcc metals as PFM.

We have investigated the effect of strain on H solubility in bcc metals of W, Mo, Fe and Cr, using first-principles calculation. Our calculations were performed using the pseudopotential plane-wave method as implemented in the VASP code [11, 12] based on the density functional theory (DFT). We used the generalized gradient approximation of Perdew and Wang [13] and projected augmented wave potentials [14], with a plane wave energy cutoff of 350 eV. The bcc supercell of 54 atoms was used and its Brillouin zone was sampled with (5×5×5) ***k***-points by the Monkhorst-Pack scheme [15]. The energy minimization is continued until the forces on all the atoms are converged to less than 10^{-3} eVÅ^{-1}. The H solution energy (E_{ε}^{sol}) in the strained metal is calculated as $E_{\varepsilon}^{sol} = E_{\varepsilon,H} - E_{\varepsilon} - \frac{1}{2}E_{H_2}$, where $E_{\varepsilon,H}$ and E_{ε} are total energies with and without H in the supercell, respectively, ε is the applied strain, and E_{H_2} is the calculated total energy of an H_2 molecule (-6.76 eV). This corresponds to the binding energy of ~4.53 eV for a H_2 molecule, consistent with the experiment [16]. Since the H atom is a light-mass particle and therefore has a high vibrational energy compared to the relatively slowly moving heavy metal atoms, the zero-point energy of H has been taken into account by summing up the zero-point vibrational energies of H's normal modes. For lattice relaxation, under hydrostatic strain, the lattice parameter is fixed at given strain values with atomic positions relaxed; under anisotropic biaxial strain, the in-plane x and y lattice parameters are fixed at given strain values, with the z-lattice parameter relaxed and optimized with

all atomic coordinates.

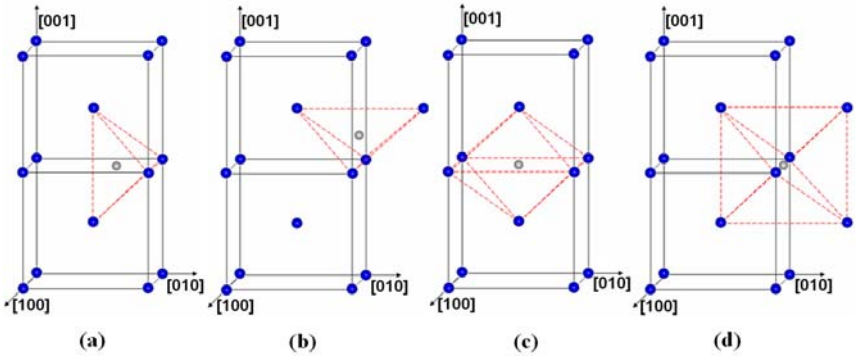

FIG. 1 (color online). The interstitial sites in a bcc lattice. (a) TIS-I, (b) TIS-II, (c) OIS-I, and (d) OIS-II. The larger blue spheres represent the metal atoms, the smaller gray sphere represents the H atom.

TABLE 1. H solution energies (in eV) and H-induced lattice stress (in GPa) in bcc metals.

			W	Mo	Fe	Cr
Solution energy		TIS	1.08	0.78	0.34	0.79
		OIS	1.48	1.03	0.44	0.92
σ	TIS-I	*XX*=*ZZ*	-0.99	-0.97	-1.25	-1.42
		YY	-0.97	-0.86	-1.10	-1.18
	TIS-II	*XX*=*YY*	-0.99	-0.97	-1.25	-1.42
		ZZ	-0.97	-0.86	-1.10	-1.18
	OIS-I	*XX*=*YY*	-0.45	-0.39	-0.91	-0.57
		ZZ	-2.21	-2.06	-2.14	-2.88
	OIS-II	*XX*	-2.21	-2.06	-2.14	-2.88
		YY=*ZZ*	-0.45	-0.39	-0.91	-0.57

When an H atom is introduced into a bcc metal lattice, it prefers to occupy an interstitial site for its small size relative to the host atom. This is confirmed by our calculations showing that in all the metals considered the H solution energy is much lower at the interstitial sites than at the substitutional site. Thus, below only the

interstitial sites will be considered. There are two kinds of interstitial sites in a bcc lattice, the tetrahedral interstitial site (TIS) and the octahedral interstitial site (OIS), as shown in Fig. 1. The TIS has four nearest neighbors (NNs) at 0.559*a*, where *a* is the lattice constant, and the OIS has six NNs, with two of them located at 0.5*a* and four at 0.707*a*. The calculated H solution energies in the equilibrium lattice are listed in Table 1. In all four metals H prefers TIS without strain, in good agreement with previous results [17-19].

A standard approach to understand the effect of strain on point defect in solid, such as H in metal, is by the concept of force dipole tensor [2]. Here, we have calculated the H-induced lattice stress tensor, which is equivalent to the force dipole tensor differing only by a volume normalization factor. Due to tetragonal lattice symmetry, at both the TIS and the OIS, the stress is anisotropic. However, the magnitude of stress anisotropy is small at the TIS but very large at the OIS, as shown in Table I.

The H behavior under strain is then dictated by the H-induced lattice stress tensor, i.e., force dipole tensor as demonstrated before [2, 3]. The defect induced lattice stress generally has two contributions [2, 3, 20]: the atomic size effect (bond deformation) and electronic band effect (Fermi level shift) termed as quantum electronic stress [20]. Typically, one assumes the stress tensor is independent of strain. Following linear elasticity theory, the H solution energy under strain can be calculated as

$$E_{\varepsilon}^{sol} = E_{\varepsilon=0}^{sol} + V(\sigma_{[100]}\varepsilon_{[100]} + \sigma_{[010]}\varepsilon_{[010]} + \sigma_{[001]}\varepsilon_{[001]}), \quad (1)$$

where $E_{\varepsilon=0}^{sol}$ is the H solution energy without strain, V is the volume of supercell at equilibrium, σ is the H-induced lattice stress in the equilibrium lattice, and ε is the

strain. Note that this equation applies to a special case of the force dipole tensor (as well as the strain tensor) that is diagonal in the chosen cubic crystal system. In applying an isotropic (hydrostatic) strain, $\varepsilon_{[100]} = \varepsilon_{[010]} = \varepsilon_{[001]}$, one expects a linear dependence of H solution on strain with a slope equals to the average stress, $\overline{\sigma} = 1/3(\sigma_{[100]} + \sigma_{[010]} + \sigma_{[001]})$. This is indeed confirmed by our DFT calculations, which show very good agreement between the prediction from Eq. (1) (solid lines), using the data of $E^{sol}_{\varepsilon=0}$ and σ in Table 1, and the direct calculations of H solution energy under different isotropic strains (data points), as shown in Fig. 2, except at

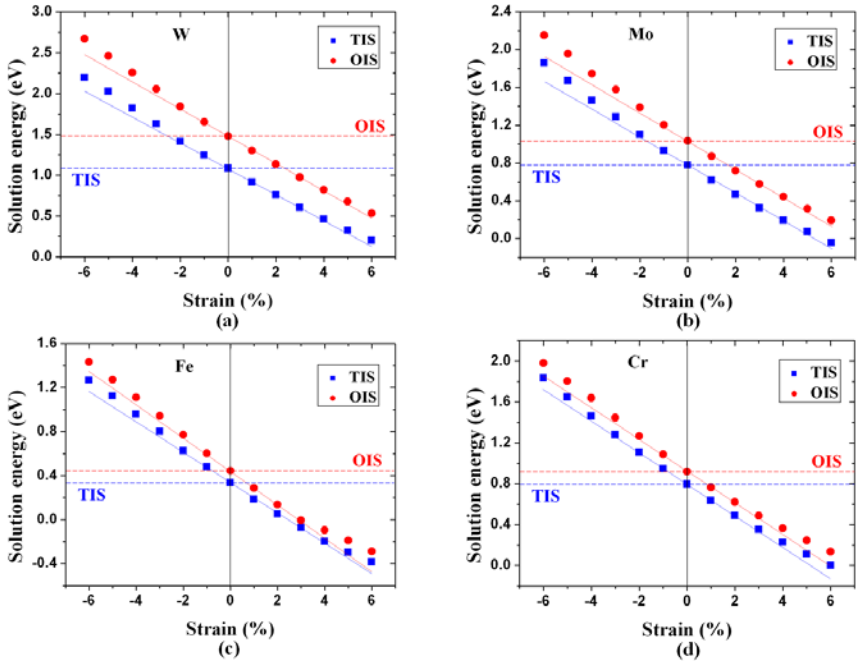

FIG. 2 (color online). The H solution energy at TIS and OIS as a function of applied hydrostatic strain. (a) W. (b) Mo. (c) Fe. (d) Cr. The solid line is the linear elasticity model prediction of Eq. (1) using the DFT data of solution energies and stresses without strain in Table I.

large strains where nonlinear effects becomes important. Because the average stress is compressive (negative by convention, see Table I), the H solution energy decreases "monotonically" in all four metals with the increasing tensile strain but increases with

the increasing compressive strain. Also, the TIS remains to be the preferred site under all strains. So, overall we may view the results under hydrostatic strain in Fig. 2 as the "normal behavior" in accordance with our common expectations [2, 3].

Next, we consider the case of applying anisotropic (biaxial) strain. When biaxial strain is applied in the x-y plane along the [100] and [010] directions (see Fig. 1), the lattice parameter along the z-direction ([001]) is fully relaxed according to Poisson ratio (ν). So, the applied strain tensor is $\varepsilon_{[100]} = \varepsilon_{[010]} = -\varepsilon_{[001]} / \nu$, with lattice contraction (expansion) in the x-y plane and expansion (contraction) along z-direction. From our calculations, we obtain the Poisson ratio 0.29, 0.28, 0.31, and 0.21 for W, Mo, Fe, and Cr, respectively. Following Eq. (1), the H solution energy should still depends linearly on the strain with a slope of $\overline{\sigma} = 1/3(\sigma_{[100]} + \sigma_{[010]} - \nu\sigma_{[001]})$. The

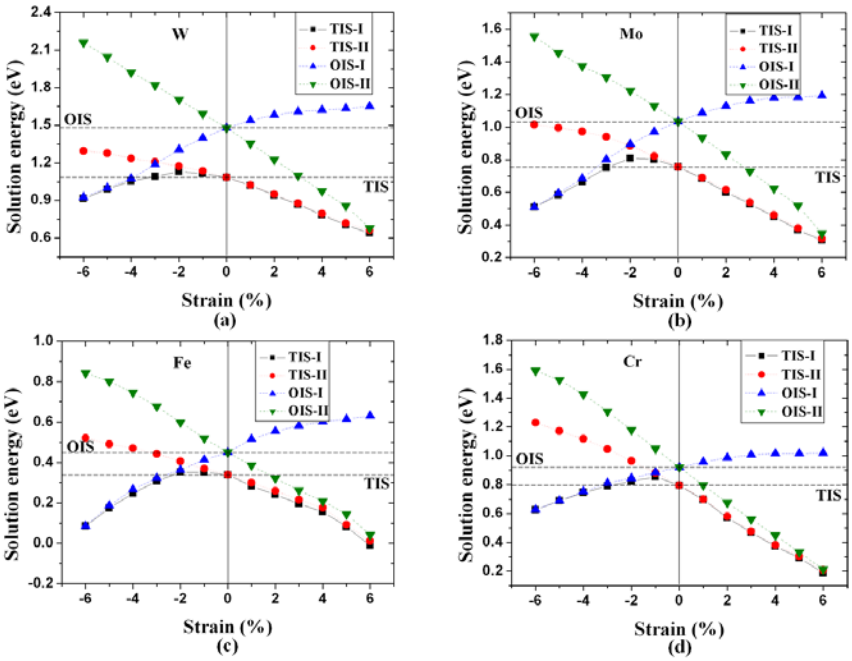

FIG. 3 (color online). The solution energy of H in bcc metals (W, Mo, Fe, and Cr) under the biaxial strain applied along the [100] and [010] directions.

calculation results under biaxial strain are presented in Fig. 3. Because the biaxial

strain breaks the lattice symmetry causing a bcc to body-centered tetragonal (bct) structural transformation, here we have to consider two different TIS and OIS configurations denoted as TIS-I, TIS-II, OIS-I, and OIS-II, respectively, in Fig. 1. The most important observation here is that the linear dependence is followed at all four locations only for very small strain but not for large strain. Also, we note that the results at the OIS-I have an opposite trend from those at other three sites. This is caused by the large stress anisotropy and Poisson effect. When compressive biaxial strains are applied in the x-y plane, a tensile uniaxial strain is applied in z-direction by Poisson ratio. Note that the stress tensor components switch by symmetry between σ_{yy} and σ_{zz} at the TIS-I and the TIS-II, and between σ_{xx} and σ_{zz} at the OIS-I and the OIS-II, respectively, as shown in Table I. Consequently, the z-component stress is much larger than x- and y-component at the OIS-I but not so at the OIS-II (see Table I), so that the z-direction effect dominates at the OIS-I to show a net tensile strain effect when compressive strain is applied in the x-y plane. (The difference between TIS-I and TIS-II is too small to show an effect.)

Overall, the results at the TIS-II and the two OIS are relatively normal showing a monotonic strain dependence of solution energy. Surprisingly, however, the TIS-I solution energy (black squares in Fig. 3) shows non-monotonic dependence on strain, especially decreasing with the increase of both signs of strain. Thus, for the TIS-I site, the standard picture of Eq. (1) with stress (force dipole) tensor [2, 3] fails. Most importantly, since the TIS-I remains to be the preferred site with lower energy than the TIS-II and the two OIS under strain (see Fig. 3), this unusual TIS-I behavior may

dominate the overall stain dependence of H solubility in bcc metals, which cannot be simply understood by the standard picture. Practically, it implies that the H solubility can be enhanced by applying either a tensile or compressive anisotropic strain!

To show the above more clearly, we plot in Fig. 4 the change of overall H solution energy in the anisotropically strained metal relative to that in the strain-free metal ($E^{dif} = E^{sol}_{\varepsilon,H} - E^{sol}_{TIS,H}$). Except for a small increase (<0.05 eV) in a limited range of

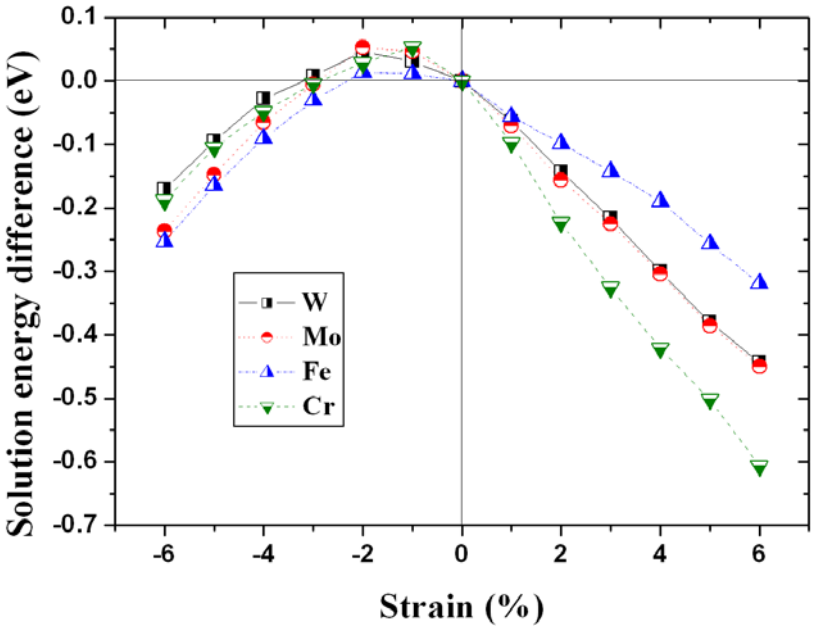

FIG. 4 (color online). Change of H solution energy vs biaxial strain in the bcc metals studied. The biaxial strain is applied along the [100] and [010] directions. Negative values indicate enhanced H solubility in the strained bcc metals for given strain values.

small compressive strain, the H solution energy decreases over a wide range of strain signs and values. This means that the H solubility can be effectively enhanced in all the strained bcc metals, almost independent of the sign of strain.

We now discuss the physical origin underlying the anomalous sign independence of H solubility on strain in bcc metals. It is important to realize that the common expectation of a monotonic dependence of H solution energy on strain has a

prerequisite condition that the stress tensor (or force dipole tensor) [2, 3] is independent of strain to guarantee the applicability of Eq. (1). This implies H to stay at the same configuration under strain, i.e., neither the site occupation, nor the location and nor the lattice displacement field induced by H change appreciably under strain. This condition is always satisfied by symmetry constraint when a hydrostatic strain is applied, as shown in Fig. 1. When a biaxial strain is applied, however, we found that this condition can break down due to the broken symmetry for H at the TIS-I. Figure 5 shows the continuous change of H minimum-energy location in W, initially placed at the TIS-I, induced by anisotropic strain discovered from our DFT

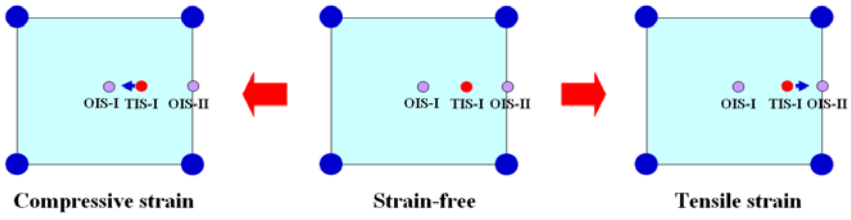

FIG. 5 (color online). The strain induced H position change starting at the TIS-I site. Compressive biaxial strain drives the H move towards left to the OIS-I site (left panel) and tensile biaxial strain drives the H move towards right to the OIS-II site (right panel).

calculations. Under compressive biaxial strain the H moves towards the OIS-I site and reaches the OIS-I at about -4% strain as seen in Fig. 3(a) beyond which the energy curves of the TIS-I and the OIS-I merge together. Under tensile biaxial strain the H moves towards the OIS-II site and reaches the OIS-II at about +6% strain as seen in Fig. 3(a) beyond which the energy curves of the TIS-I and the OIS-II merge together. Therefore, it is such unusual strain induced change of H position that is responsible for the observed anomalous non-monotonic dependence of H solution energy on strain, leading to the end result of energy decreasing under both signs of strain.

Apparently, such strain induced change of microscopic atomic configuration cannot be captured by the macroscopic continuum elasticity theory. Similar behaviors of H under biaxial strain are also found in other bcc metals of Mo, Fe, and Cr, which leads to anomalous non-monotonic strain dependence of H solution energy in all four bcc metals studied as shown in Fig. 4.

We note that the previous work has shown that H in bcc metals can switch from TIS to OIS as a function of isotopic mass [21]. Here, we discover a different mechanism for H switching from TIS to OIS as a function of anisotropic strain. The isotope effect changes the relative stability of TIS versus OIS, and hence the relative H population between the two sites. Instead, the anisotropic strain moves the minimum-energy H position gradually from TIS to OIS with the increasing strain; at the intermediate strain, the minimum-energy position sits in between the TIS and OIS. Simple nearest-neighbor H-Metal interaction model [22] may suggest the change of relative stability of TIS vs. OIS under anisotropic strain but cannot resolve such a complex evolution of potential-energy surface versus strain.

Our finding indicates that inside a non-uniformly strained bcc metal, H is favored to dissolve into either compressive or tensile strained regions except for a small range of compressive strain values. This has an important implication in using bcc metals as PFM in a nuclear reactor. In particular, W has been considered as the most promising PFM, but H blistering in W-PFM seriously influences the plasma stability and limits the lifetime of W-PFM. H blistering is also a major concern in the fusion research. As such, many studies have been devoted to find ways to suppress H bubble formation in

W [23-25]. The internal gas pressure in H bubbles is estimated up to a few tens of GPa [26, 27], and thus H bubbles will exert a large strain to the surrounding W lattice, so that elastic strain is believed an important factor in affecting the H bubble formation [28]. However, the physical mechanism underlying the relationship between strain and H bubble formation remains poorly understood, and no microscopic insight has been given so far. Here, we propose that there exists a strain-triggered cascading effect on H bubble formation in bcc metals: the H solution leads to H bubble formation that induces anisotropic strain in the W lattice around the bubble, which in turn enhances local H solubility that facilitates further growth of H bubble.

In particular, H bubble is observed to form in the surface regions after W is exposed to H plasma irradiation [27, 29], to adopt different size and shape depending on the microstructure of W crystal target and the irradiation temperature. Therefore, the strain in the W lattice surrounding the H bubble must be highly non-uniform and anisotropic due to the low-symmetry surface environment and the irregular size and shape of H bubble. According to our study, such anisotropic strain field will drive more H atoms to segregate into the vicinity of H bubbles, even independent of the sign of strain for most strain values; and the larger the anisotropic strain is, the lower the H solution energy will be. The increased H concentration will then facilitate further growth of H bubble, and as the bubble grows bigger it induces even larger anisotropic strain around it which in turn attracts more H to make the bubble grow even bigger, resulting into a cascading effect.

This research is supported by National Magnetic Confinement Fusion Program with Grant No. 2009GB106003 and National Natural Science Foundation of China (NSFC) with Grant No. 51061130558. F. Liu thanks support by DOE-BES (Grant No. DE-FG02-04ER46148) and NSF-MWN (Grant No. DMR0909212) program.

*LGH@buaa.edu.cn

[1] G. Leibfried and N. Breuer, "Point Defects in Metals I: Introduction to Theory", in Springer Tracts in Modern Physics, Vol. 81 (Springer-Verlag, New York, 1978).

[2] C. Elsässer, M. Fähnle, L. Schimmele, C. T. Chan, and K. M. Ho, Phys. Rev. B **50**, 5155 (1994).

[3] J. Y. Zhu, F. Liu, G. B. Stringfellow, and S. H. Wei, Phys. Rev. Lett. **105**, 195503 (2010).

[4] S. M. Myers, M. I. Baskes, H. K. Birnbaum, J. W. Corbett, G. G. DeLeo, S. K. Estreicher, E. E. Haller, P. Jena, N. M. Johnson, R. Kirchheim, S. J. Pearton, and M. J. Stavola, Rev. Mod. Phys. **64**, 559 (1992).

[5] Y. Fukai and N. Okuma, Phys. Rev. Lett. **73**, 1640 (1994).

[6] Y. Fukai, Phys. Scr. **T103**, 11 (2003).

[7] P. Chen, Z. T. Xiong, J. Z. Luo, J. Y. Lin, and K. L. Tan, Nature (London) **420**, 302 (2002).

[8] S. Li, P. Jena, and R. Ahuja, Phys. Rev. B **73**, 214107 (2006).

[9] A. R. Troiano, Trans. Am. Soc. Met. **52**, 54 (1960).

[10] J. B. Condon and T. J. Schober, J. Nucl. Mater. **207**, 1 (1993).

[11] G. Kresse and J.Hafner, Phys. Rev. B **47**, 558 (1993).

[12] G. Kresse and J. Furthmüller, Phys. Rev. B **54**, 11169 (1996).

[13] J. P. Perdew and Y. Wang, Phys. Rev. B **45**, 13244 (1992).

[14] P. E. Blöchl, Phys. Rev. B **50**, 17953 (1994).

[15] H. J. Monkhorst and J. D. Pack, Phys. Rev. B **13**, 5188 (1976).

[16] K. P. Huber and G. Hertzberg, Molecular Spectra and Molecular Structure IV: Constants of Diatomic Molecules (Van Norstrand Reinhold, New York, 1979).

[17] Y. L. Liu, Y. Zhang, H. B. Zhou, G. H. Lu, F. Liu, and G. N. Luo, Phys. Rev. B **79**, 172103

(2009).

[18] C. Duan, Y. L. Liu, H. B. Zhou, Y. Zhang, S. Jin, G. H. Lu, and G.-N. Luo, J. Nucl. Mater. **404**, 109 (2010).

[19] Y. A. Du, L. Ismer, J. Rogal, T. Hickel, J. Neugebauer, and R. Drautz, Phys. Rev. B **84**, 144121 (2011).

[20] H. Hu, M. Liu, Z. F. Wang, J. Zhu, D. Wu, H. Ding, Z. Liu, and F. Liu, Phys. Rev. Lett. **109**, 055501 (2012).

[21] H. Krimmel, L. Schimmele, C. Elsässer, and M. Fähnle, J. Phys.: Condens. Matter **6**, 7705 (1994).

[22] R. Griessen, Phys. Rev. B **38**, 3690 (1988).

[23] H. B. Zhou, Y. L. Liu, J. Shuo, Y. Zhang, G. N. Luo, and G. H. Lu, Nucl. Fusion **50**, 115010 (2010).

[24] O. V. Ogorodnikova, T. Schwarz-Selinger, K. Sugiyama, and V. K. Alimov, J. Appl. Phys. **109**, 013309 (2011).

[25] M. J. Baldwin, R. P. Doerner, W. R. Wampler, D. Nishijima, T. Lynch, and M. Miyamoto, Nucl. Fusion **51**, 103021 (2011).

[26] A. V. Veen, H. A. Filius, J. D. Vries, K. R. Bijkerk, G. J. Rozing, and D. Segers, J. Nucl. Mater. **155**, 1113 (1988).

[27] W. M. Shu, E. Wakai, and T. Yamanishi, Nucl. Fusion **47**, 201 (2007).

[28] M. Balden, S. Lindig, A. Manhard, and J. H. You, J. Nucl. Mater. **414**, 69 (2011).

[29] R. A. Causey and T. J. Venhaus, Phys. Scr. **T94**, 9 (2001).